Cross-platform Profiling of ctDNA Using ddPCR: Standardization of the Liquid Biopsy for Pediatric Diffuse Midline Glioma

Daphne Li
Loyola University Chicago Stritch School of Medicine
Erin R Bonner
Children's National Medical Center: Children's National Health System
Kyle Wierzbicki
University of Michigan
Eshini Panditharatna
Harvard University
Tina Huang
Northwestern University Feinberg School of Medicine
Rishi Lulla
Brown University
Sabine Mueller
University of California San Francisco
Carl Koschmann
University of Michigan
Javad Nazarian
Children's National Medical Center: Children's National Health System
Amanda Muhs Saratsis (asaratsis@luriechildrens.org)
Division of Pediatric Neurosurgery Department of Surgery Ann & Robert H. Lurie Children's Hospital of Chicago
https://orcid.org/0000-0002-4913-2771

Research

Keywords: diffuse midline glioma, liquid biopsy, digital droplet PCR, H3K27M, tumor biomarkers, circulating tumor DNA

Posted Date: September 16th, 2020

DOI: https://doi.org/10.21203/rs.3.rs-75571/v1

Abstract

Background

Diffuse midline glioma (DMG) is a highly morbid pediatric brain tumor. Up to 80% of DMGs harbor mutations in histone H3-encoding genes, associated with poorer prognosis. We previously showed the feasibility of detecting H3 mutations in circulating tumor DNA (ctDNA) in the liquid biome of children diagnosed with DMG. However, detection of low ctDNA concentrations is highly dependent on platform sensitivity and sample type. To address this, we optimized ctDNA detection sensitivity and specificity across two commonly used digital droplet PCR (ddPCR) platforms (RainDance and BioRad), and validated methods for detecting *H3F3A* mutations in DMG CSF, plasma, and primary tumor specimens across three different institutions.

Methods

DNA was extracted from H3.3K27M mutant and H3 wildtype (H3WT) specimens, including H3.3K27M tumor tissue (n=4), CSF (n=6), plasma (n=4), and human primary pediatric glioma cells (H3.3K27M, n=2; H3WT, n=1). ctDNA detection was enhanced via PCR pre-amplification and use of distinct custom primers and fluorescent LNA probes for c.83 AàT *H3F3A* mutation detection. Mutation allelic frequency (MAF) was determined and validated through parallel analysis of matched H3.3K27M tissue specimens (n=3).

Results

We determined technical nuances between ddPCR instruments, and optimized sample preparation and sequencing protocols for *H3F3A* mutation detection and quantification. We observed 100% sensitivity and specificity for mutation detection in matched DMG tissue and CSF across assays, platforms and institutions

Conclusion

Our study demonstrates that ctDNA is reliably and reproducibly detected in ctDNA using ddPCR, representing a clinically feasible and reproducible minimally invasive approach for DMG diagnosis, molecular subtyping and therapeutic monitoring.

Background

Diffuse midline glioma (DMG) is a highly morbid pediatric central nervous system (CNS) tumor for which there is currently no effective treatment. Approximately 20% of pediatric CNS tumors occur in the brainstem, of which up to 80% are DMG (1). Due to their anatomic location and infiltrative nature, DMGs are not amenable to surgical resection and are most often diagnosed radiographically and treated with radiation therapy, with no effect on survival (2–5). Recent studies of DMG biology revealed distinct genomic alterations compared to hemispheric pediatric and adult gliomas (2, 3). Specifically, 80% of pediatric DMGs harbor somatic mutations in histone H3-encoding genes *H3F3A* (60%), *HIST2H3C* or *HIST1H3B/C* (20%), resulting in lysine-27-to-methionine (H3K27M) conversion that confers a more aggressive clinical course and poorer overall response to therapy (6–12). As such, the World Health Organization (WHO) classified H3K27M mutant DMG as a distinct clinical entity in 2016, with the biological and clinical implications of H3K27M mutation making detection critical for diagnosis, treatment, and clinical trial enrollment (13–15). While clinically feasible, stereotactic tumor tissue biopsy for mutation detection is not without significant surgical risk (16). Further, tumor response to therapy is typically monitored using serial conventional MRI, making discerning pseudo-progression from progressive disease challenging. In contrast, tumor “liquid biopsy” via cerebrospinal fluid (CSF) or blood sampling may represent a more clinically feasible, less invasive approach for evaluating tumor biology and treatment response (17).

It is crucial for clinicians and scientists to consider new technical approaches as the molecular understanding and treatment of DMG evolves. We previously reported *H3F3A* c.83 A–>T (H3.3K27M) mutation detection in circulating tumor DNA (ctDNA) in CSF and plasma from children with DMG, and developed a digital droplet PCR (ddPCR) approach to detect and monitor H3K27M in ctDNA from the DMG liquid biome(17–19). This work, and mounting evidence in the literature, demonstrate liquid biopsy as a viable tool for clinicians to diagnose and monitor pediatric CNS tumors(20). Clinical implementation of this approach requires exquisite test reliability, sensitivity and specificity, but differences in ddPCR instruments and protocols impede broad clinical application of this technique. Additionally, poor access to specimens further exacerbates the challenge of validating and optimizing these analytic methods for this rare tumor.

To address these challenges, we optimized our ddPCR-based technique for H3.3K27M detection using matched DMG tissue and liquid biopsy specimens, and validated our approach across three academic institutions using two leading ddPCR instruments. Here, we show high test sensitivity, specificity, and reproducibility for detecting and quantifying H3.3K27M-mutant ctDNA across institutions and platforms, which is essential for clinical implementation of this powerful new approach.

Methods

Biological Specimens

Patient specimens (Table 1) were collected during the course of treatment (PNOC003, NCT02274987) or upon autopsy, after informed consent as approved by Institutional Review Boards (Lurie Children's Hospital of Chicago 2012–14877 and 2005–12252, Northwestern University STU00202063, University of California San Francisco 14-13895, University of California San Diego 150450, and Children's National Health System 1339, 747). All patient identifiers were removed with de-identified numerical identifiers assigned.

Table 1
Custom, sequence specific primers and fluorescent locked nucleic acid (LNA) probe sets utilized.

	Assay A (Pandarithna et al, CN)	**Assay B (Stallard et al, UM)**	**Assay C (Huang et al, NU)**
Forward Primer	5'-GTACAAAGCAGACTGCCCGCAAAT-3'	5'-GGTAAAGCACCCAGGAAG-3'	5'-TGCTGGTAGGTAAGTAAGGAG-3'
Reverse Primer	5'-GTGGATACATACAAGAGAGACTTTGTCCC-3'	5'-CAAGAGAGACTTTGTCCC-3'	5'-CAAGAGAGACTTTGTCCC-3'
Wild-type Probe	/5HEX/CA + C + T + C + T + T + GC/3IABkFQ/	5'-HEX-TC + GC + A + A + GA + GT + GC-IABkFQ-3'	n/a (used only primers for pre-amplification)
Mutant Probe*	/56-FAM/CA + CT + C + **A** + T + GCG/3IABkFQ/	5'-6-FAM-TC + GC + A + **T** + GA + GTGC-IABkFQ-3'	
ddPCR Amplicon	173 bp	130 bp	300 bp
*mutant base is bold, "+" denotes LNA bases			
† Used only primers for preamplification			
Abbreviations: HEX: hexachlorofluorescein, 6-FAM: 6-carboxyfluorescein, IABkFQ: Iowa Black® FQ quencher			

CSF from children with brain tumors (n = 5, Table 1) was collected during the course of treatment or at autopsy. CSF from a patient with congenital hydrocephalus was used as negative control. CSF specimens were centrifuged at 500 *x g* for five

minutes at 4 °C (NU), or at 5,000 *x g* for 10 minutes at 4 °C (CN) via established institutional biobanking protocols. The resulting cell-free supernatant was collected, aliquoted, and stored at -80^{o}C.

Plasma or serum was collected from patients with DMG enrolled in the PNOC003 at the time of diagnosis (NCT02274987) or at autopsy (n = 4) (Table 1**)**. Whole blood was collected in purple top potassium EDTA tubes for plasma isolation, inverted and spun at 2,000 *x g* for 15 minutes at 4^{o}C. For serum samples, blood was collected in gel-barrier tubes with clot activator and gel and incubated at room temperature for 30 minutes. Blood was centrifuged to separate plasma/serum (supernatant), white blood cells, and red blood cells pellet. Plasma/serum was aliquoted into cryovials and stored at -80^{o}C.

Tumor tissue was obtained from DMG patients during the course of treatment or at autopsy (n = 4) and stored at -80^{o}C. H3K27M status was validated via DNA sequencing **(Additional** Table 1**)**. Pediatric glioma cell lines SF7761 (H3.3K27M DIPG) and KNS42 (H3.3G34V supratentorial pediatric high-grade glioma, were cultured as previously described and used for analysis (**Additional** Table 1) (12, 21, 22).

DNA extraction

QIAamp DNA Mini Kit (Qiagen) was used to extract genomic DNA (gDNA) from 5×10^6 cells per manufacturer's protocol. Tumor tissue gDNA was extracted using Gentra Puregene tissue kit (Qiagen) according to manufacturer's instructions. ctDNA was extracted from 1 mL plasma using the QIAmp Circulating Nucleic Acid Kit (Qiagen) per manufacturer's protocol. Qiagen protocol for purification of circulating nucleic acids from 1 mL of urine was used to extract ctDNA from 500 µL of CSF. ctDNA was eluted in 100 µL buffer AVE or MB grade H_2O twice in order to increase DNA yield. Extracted gDNA and ctDNA were quantified using Nanodrop Nucleic Acid Quantification (Thermo Fisher Scientific) and Qubit Fluorometric Quantitation (Thermo Fisher Scientific).

DNA PCR Pre-amplification

gDNA extracted from tumor tissue and cells, and ctDNA extracted from CSF and plasma, was pre-amplified at CN using Q5 hot start high-fidelity master mix (New England Biolabs), and at NU using SsoAdvanced PreAmp Supermix (Biorad), with 50 nmol/L each of forward and reverse primer. Pre-amplification at CN was performed using Assay A primers (**Additional** Fig. 1) in ABI 2720 thermocycler: 98 °C for 3 minutes; nine cycles of 98 °C for 10 seconds, 58 °C for 3 minutes, 72 °C for 30 seconds; and an extension of 72 °C for 2 minutes. Product was diluted 1:5 with TE buffer (pH 8.0). Pre-amplification at NU was performed on the BioRad T100 thermocycler using the following conditions: 95 °C for 3 minutes, 10 cycles of 95 °C for 15 seconds, annealing temperature (58 °C) for 4 minutes. The pre-amplified product was diluted 1:5 with molecular grade water. At CN, 0.025 ng gDNA from DIPG-51-T was used as a positive control per a previously established institutional protocol(17, 19). 2 ng of tumor gDNA was used for ddPCR analysis of patient-matched tumor, CSF and plasma/serum specimens. Where applicable, starting ctDNA aliquots were speed-vacuum concentrated from 100 µL to 10.5–11 µL prior to pre-amplification. Assay A primers were used for ctDNA pre-amplification of all samples at CN, while Assay C primers were used for PCR pre-amplification at NU (18).

ddPCR Analysis

Custom sequence-specific primers and fluorescent locked nucleic acid (LNA) probes for *H3F3A* amplification and sequencing were used based on previously reported assay designs by collaborating institutions (Table 1, **Additional** Fig. 1) (18, 19, 23). ddPCR reactions at CN were conducted using RainDrop according to manufacturer instructions (RainDance Technologies). ddPCR was conducted with 1x TaqMan Genotyping Mastermix (Life Technologies), 1xRainDance droplet stabilizer, 12 µL target DNA product, 900 nmol/L forward and reverse primers, and 200 nmol/L mutant and wildtype probes. The following ddPCR protocol was used: 1 cycle at 95 °C for 10 minutes, 45 cycles at 95 °C for 30 seconds and 58 °C for 2 minutes, 1 cycle at 98 °C for 10 minutes, and 1 cycle at 10 °C infinite, all at a ramp rate of 0.5 °C/second.

ddPCR reactions performed at NU and UM were conducted using BioRad Q200 according to the manufacturer's instructions. ddPCR reactions were conducted with 2x ddPCR Supermix for probes (BioRad, no dUTP), 1–5 µL of target DNA product, 900 nmol/L of forward and reverse primers, and 200 nmol/L of mutant and wildtype probes. The following ddPCR protocol was used at UM: 1 cycle at 95 °C for 10 minutes, 40 cycles at 94 °C for 30 seconds and 58 °C for 1 minute, 1 cycle at 98 °C for 10 minutes, and 1 cycle at 12 °C infinite, all at a ramp rate of 2 °C/second. Since Assay A was originally designed for the RainDance platform, a modified ddPCR thermocycling protocol was employed to optimize droplet detection and results on the BioRad platform at NU. The ddPCR protocol employed was: 1 cycle at 95 °C for 10 minutes, 45 cycles at 95 °C for 30 seconds and 58 °C for 2 minutes, 1 cycle at 98 °C for 10 minutes, and 1 cycle at 10 °C infinite, all at a ramp rate of 2 °C/second. All plasma and CSF samples were analyzed in technical duplicate or triplicate based on sample availability.

Statistical Analysis

Data generated on BioRad Q200X was analyzed with Quantasoft AnalysisPro, while data generated on RainDrop was analyzed with RainDrop Analyst II (17). Mutation allelic frequency (MAF) for each sample was calculated as follows: number positive mutant droplets detected / (number positive mutant droplets detected + number positive wild type droplets detected). Poisson-corrected droplet counts were used to calculate MAF. Nonparametric tests were employed for results analysis. All data points represent technical duplicates or triplicates based on sample availability. Paired samples were analyzed by Wilcoxon signed-rank test, unpaired analyzed by Mann–Whitney test. Threshold for false positive droplets was based on non-template control samples analyzed with test samples in each assay, with false positive droplets accounted when calculating MAF. For all analyses, a p-value < 0.05 defined statistical significance.

Results

Optimization of ctDNA droplet detection

We compared two PCR primer and probe sets, developed at two participating institutions, in order to determine optimal ddPCR reaction conditions (Table 1, **Additional** Fig. 1). For CSF ctDNA analysis, we detected fewer false positive droplets with Assay A on the BioRad platform (Fig. 1A-B), which may be attributed to the shorter length of Assay A probes improving the specificity of probe-target DNA hybridization. No significant difference in CSF droplet counts or MAFs were observed between assays on the RainDance platform (Fig. 1C). On the BioRad platform, Assays A and B resulted in similar droplet counts, but B resulted in lower MAF due to poorer separation between wildtype, mutant and negative clusters compared to A (**Additional** Fig. 2A**)**. To ameliorate this issue, gating adjustments were tailored to ensure maintenance of droplet non-detection on non-template control samples, while maximizing positive wildtype droplet detection in target reaction wells. In contrast, distinct separation of negative, wildtype and mutant droplet clusters was achieved using both assays on the RainDance (**Additional** Fig. 2B). False positive droplets did not exceed 5 droplets per sample on the BioRad platform, and fewer false positives were detected on the RainDance platform. Droplet separation was optimized at 58^{O}C (**Additional** Fig. 3A). Increasing thermocycling to 45 cycles improved separation without increasing false positives, and was used for all subsequent ddPCR analyses with Assay A at NU **(Additional** Fig. 3B**)**.

ctDNA pre-amplification increases ddPCR sensitivity

We tested the effect of ctDNA pre-amplification on ddPCR assay sensitivity (Fig. 1). H3.3K27M mutant (DIPG-1-C) and H3WT CSF (H-C) were analyzed with non-template controls on the BioRad platform as follows: 1) no pre-amplification; 2) PCR pre-amplification with primers used for subsequent ddPCR; or 3) PCR pre-amplification with Assay C primers, and subsequent ddPCR with Assay A or B primers (Fig. 1A-B, **Additional** Fig. 2A). We detected greater mutant droplets and MAF values with pre-amplification, regardless of PCR primers used, with no change in test specificity. False positive mutant droplet detection in the H3WT sample was observed after Assay B PCR pre-amplification and ddPCR analysis, but was not statistically significant.

RainDance was used to test similar workflows for H3.3K27M mutant CSF analysis (DIPG-70-C): 1) no pre-amplification; or 2) pre-amplification with Assay A followed by ddPCR with either Assay A or B (Fig. 1C, **Additional** Fig. 2B). Again, more mutant droplets and greater MAF values were observed with ctDNA pre-amplification regardless of PCR primers used, with no change in test specificity. ddPCR analysis results were not affected by the specific primers used for PCR pre-amplification, as long as primers used for subsequent ddPCR were identical to, or nested within, the pre-amplification primer amplicon (Table 1, **Additional** Fig. 1).

Optimizing low ctDNA detection

To optimize mutation detection in low starting [ctDNA], we isolated, concentrated and pre-amplified ctDNA from CSF (DIPG-70-C) and plasma (DIPG-168-P), then tested on RainDance (CN) and BioRad (NU) platforms (Fig. 2, **Additional** Fig. 4). Importantly, we detected positive mutant droplets in all specimens, across all platforms and institutions, with no statistically significant difference in calculated MAF **(**Fig. 2, **Additional** Fig. 4**)**. Speed vacuum-concentration of pre-amplified ctDNA further increased the number of positive droplets detected **(Additional** Fig. 4**)**. We observed a statistically significant difference in calculated MAFs between Assay A and B ddPCR primer sets on the BioRad platform, due to poorer separation of positive and negative droplets with Assay A. Because the RainDance instrument can accommodate 12 µL sample input compared to 1–5 µL on BioRad, we found vacuum-concentration was necessary to ensure equivalent input [ctDNA] between platforms (Fig. 2B, **Additional** Fig. 4). There was no statistically significant difference in calculated MAFs between the samples analyzed on the RainDance versus speed-vacuum concentrated specimens the BioRad instrument (Fig. 2**)**.

Cross-platform ddPCR validation with patient-matched samples

To demonstrate reproducibility of our findings across ddPCR platforms, we analyzed matched tumor tissue, CSF and blood specimens from three patients with tissue-validated H3.3K27M mutant DMG (DIPG-26, DIPG-73, DIPG-128, Fig. 3, **Additional Fig. 5A, B)**. Tissue gDNA and liquid specimen ctDNA was extracted, concentrated and pre-amplified at one site (CN) to minimize technical variability, then analyzed on RainDance (CN) and BioRad platforms (NU). Samples were analyzed using Assay A, given greater assay sensitivity and specificity (Fig. 1). H3.3K27M was detected in all samples tested, with fewer positive droplets in blood samples compared to CSF and tissue. MAF values were higher on BioRad, likely due to the noted differences in wildtype droplet separation using Assay A **(Additional Fig. 5A).**

Cross-platform ddPCR validation by specimen origin

All samples were prepared at CN prior to the analyses described above. In these studies, comparable positive droplet counts were observed with both assays on a given platform, but more mutant droplets were consistently detected on RainDance. To determine whether this difference was due to DNA loss associated with sample shipping and handling or the ddPCR instrument itself, we also extracted and quantified DNA from tissue-validated H3.3K27M DMG mutant CSF (DIPG-1-C) and cells SF7761 at NU. Cell gDNA (2 ng) and CSF ctDNA (16 ng) were pre-amplified using Assay C primers, and paired aliquots were analyzed on BioRad (NU) or shipped for analysis on RainDance (CN). Greater positive droplets were detected on the RainDance, regardless of the assay set used for ddPCR, with no difference in calculated MAF between platforms regardless of sample origin and shipment (Fig. 4).

Discussion

Pediatric DMG is universally fatal, with a high rate of histone H3 mutations. We previously demonstrated histone H3 variant detection in DMG ctDNA from CSF and plasma, allowing longitudinal monitoring of changes in ctDNA level in liquid biopsy specimens without the need for repeated tumor tissue biopsy (17–19, 23–25). Given this potential clinical impact, we sought to optimize and validate our approach across multiple institutions and ddPCR platforms. This multi-institutional collaboration was critical, given the paucity of DMG specimens available for study and need for broadening clinical application across institutions, particularly as the RainDance instrument is no longer commercially available. By pooling resources and testing different instruments, we optimized mutant droplet identification in specimens with very low starting

[DNA], and identified technical nuances between systems. As a result, we show ddPCR of liquid biopsy specimens could be reliably and robustly employed at multiple institutions, potentially making ctDNA-based mutation profiling a reality for more patients.

Overall, we found H3.3K27M mutation detection in blood specimens to be the most technically challenging due to very low starting [ctDNA]. To overcome this challenge, we employed vacuum-concentration of pre-amplified ctDNA, which increased test sensitivity without decreasing specificity (Fig. 2B, **Additional** Fig. 3), enabling target mutation detection in patient-matched tumor tissue, CSF and blood specimens (Fig. 3). It is important to note that few mutant droplets may be identified, with the lower limit of H3.3K27M detection in our previous study as low as 0.001% MAF (**Additional Fig. 5**): indeed, blood from patients with CNS tumors is known to harbor low levels of ctDNA relative to other tumor types, requiring exquisitely sensitive methods for mutation detection (26). Despite this challenge, our work demonstrates the clinical feasibility and reliability of this approach.

Importantly, we also show ddPRCR results are not hindered by the location of sample collection, processing, or analysis (Fig. 4). This has significant implications when developing protocols for clinical specimen analysis locally or at a collaborating institution. Given that few institutions currently have access to a ddPCR instrument, the work presented here can guide protocol development for collaborative specimen sharing to inform clinical trials and improve patient treatment, without constraints imposed by geographical location and specimen access. Indeed, these findings support liquid biopsy as a rapid, cost-effective and minimally invasive method for H3K27M mutation detection and monitoring(25). The application of this precision medicine-based approach could help overcome current limitations for effective DMG treatment, including scarcity of tissue for molecular study. Further, detection of low-frequency tumor mutations using DNA from clinically accessible sources could enable validation of individualized, pre-clinical models for real time evaluation of patient response to specific therapies. Future work should be directed towards incorporating ddPCR of paired tissue and liquid specimens in prospective, longitudinal, cohort cross-sectional studies. Lastly, while our approach was optimized for *H3F3A* mutation detection in DMG, a similar platform could be tailored to investigate prognostic mutations in other cancers. As our knowledge of tumor molecular signatures expands, liquid biopsy may prove to be an increasingly valuable, broadly applicable tool in the armamentarium of precision medicine to improve patient care and clinical outcomes.

Conclusion

We present an optimized, tissue-validated ddPCR workflow to identify and quantify H3K27M-mutant ctDNA in clinically accessible CSF and plasma specimens from DMG patients. Our results demonstrate that this approach is sensitive, specific, and reproducible across multiple institutions and technical platforms. This approach could therefore have significant utility for monitoring response to therapy and improving patient care.

Abbreviations

CSF
cerebrospinal fluid
CN
Children’s National Health System
CNS
central nervous system
ctDNA
circulating tumor DNA
ddPCR
digital droplet PCR
gDNA

genomic DNA
MAF
mutant allelic frequency
NU
Northwestern University
DMG
diffuse midline glioma
UM
University of Michigan

Declarations

Ethics approval and consent to participate

All patient specimens were collected during the course of treatment (PNOC003, NCT02274987) or upon autopsy, after informed consent was obtained as approved by the Institutional Review Boards for Ann & Robert H. Lurie Children's Hospital of Chicago, Northwestern University (Lurie 2012–14877 and 2005–12252, NU STU00202063), the University of California San Francisco (San Francisco, CA; IRB #14-13895), University of California San Diego (San Diego, CA; IRB #150450), and Children's National Health System (IRB #1339, #747). All patient identifiers were removed at the time of specimen collection, with a de-identified numerical identifier assigned to each specimen before processing. Histone mutation status of each subject was confirmed by molecular analysis of tumor tissue.

Consent for publication

Not applicable.

Availability of data and materials

The sequences of all probes and primer sets used for the current study are included in the published article in Table 1. The raw ddPCR data generated and analyzed during the current study are available from the corresponding author on reasonable request.

Competing interests

The authors declare that they have no competing interests.

Funding

This work was supported by funding from the Isabella Kerr Molina Foundation, Smashing Walnuts Foundation (Middleburg, VA), the V Foundation (Atlanta, GA), The Gabriella Miller Kids First Data Resource Center, Musella Foundation (Hewlett, NY), Matthew Larson Foundation (Franklin Lake, NJ), The Lilabean Foundation for Pediatric Brain Cancer Research (Silver Spring, MD), the Children's Brain Tumor Tissue Consortium (Philadelphia, PA), Rally Foundation for Childhood Cancer Research (Atlanta, GA), the John McNicholas Pediatric Brain Tumor Foundation (Chicago, IL), the Pediatric Cancer Research Foundation (Irvine,CA), Northwestern University Clinical and Translational Sciences Institute (Chicago, IL), the Faculty Practice Plan of Ann & Robert H. Lurie Children's Hospital of Chicago (Chicago, IL), and the Northwestern Memorial Faculty Foundation (Chicago, IL). Research reported in this publication was supported, in part, by the National Institutes of Health's National Center for Advancing Translational Sciences, Grant Numbers UL1TR001422 and KL2TR001424, and the National Institute of Neurological Disorders and Stroke Grant Number K08NS097624. The content is solely the responsibility of the authors and does not necessarily represent the official views of the National Institutes of Health.

Authors' contributions

DL and ERB are co-first authors having performed the majority of sample preparation, experimental design, DNA extraction, and ddPCR analysis. DL, ERB and AMS were major contributors in data analysis and writing the manuscript. KW, EP, RH contributed to ddPCR analysis and data analysis. RL and SM contributed specimens and cell lines for analysis. CK contributed materials and supplies for ddPCR analysis. JN and AMS are co-principal investigators having contributed to the majority of experimental design and review of the manuscript. All authors read and approved the final manuscript.

Acknowledgements

The authors would like to thank all patients and their families who contributed specimens to support this research.

References

1. Walker DA, Punt JA, Sokal M. Clinical management of brain stem glioma. Arch Dis Child. 1999;80(6):558–64.
2. Bartels U, Hawkins C, Vézina G, Kun L, Souweidane M, Bouffet E. Proceedings of the diffuse intrinsic pontine glioma (DIPG) Toronto Think Tank: advancing basic and translational research and cooperation in DIPG. J Neurooncol. 2011;105(1):119–125.
3. Jansen MHA, van Vuurden DG, Vandertop WP, Kaspers GJL. Diffuse intrinsic pontine gliomas: A systematic update on clinical trials and biology. Cancer Treat Rev. 2012;38(1):27–35.
4. Falzone L, Salomone S, Libra M. Evolution of Cancer Pharmacological Treatments at the Turn of the Third Millennium. Front Pharmacol. 2018;9:1300.
5. Gojo J, Pavelka Z, Zapletalova D, Schmook MT, Mayr L, Madlener S, et al. Personalized Treatment of H3K27M-Mutant Pediatric Diffuse Gliomas Provides Improved Therapeutic Opportunities. Front Onc. 2020;9:1436.
6. Gielen GH, Gessi M, Hammes J, Kramm CM, Waha A, Pietsch T. H3F3A K27M mutation in pediatric CNS tumors: a marker for diffuse high-grade astrocytomas. Am J Clin Pathol. 2013;139(3):345.
7. Schwartzentruber J, Korshunov A, Liu X, Jones DTW, Pfaff E, Jacob K, et al. Driver mutations in histone H3.3 and chromatin remodelling genes in paediatric glioblastoma. Nature. 2012;482(7384):226.
8. Wu G, Diaz AK, Paugh BS, Rankin SL, Ju B, Li Y, et al. The genomic landscape of diffuse intrinsic pontine glioma and pediatric non-brainstem high-grade glioma. Nat Genet. 2014;46(5):444–50.
9. Saratsis A, Kambhampati M, Snyder K, Yadavilli S, Devaney J, Harmon B, et al. Comparative multidimensional molecular analyses of pediatric diffuse intrinsic pontine glioma reveals distinct molecular subtypes. Acta Neuropathol. 2014;127(6):881–95.
10. Saratsis AM, Yadavilli S, Magge S, Rood BR, Perez J, Hill DA, et al. Insights into pediatric diffuse intrinsic pontine glioma through proteomic analysis of cerebrospinal fluid. Neuro Oncol. 2012;14(5):547–60.
11. Bender S, Tang Y, Lindroth A, Hovestadt V, Jones DW, Jones C, et al. Reduced H3K27me3 and DNA Hypomethylation Are Major Drivers of Gene Expression in K27M Mutant Pediatric High-Grade Gliomas. Cancer Cell. 2013;24(5):660–72.
12. Chan K, Fang D, Gan H, Hashizume R, Yu C, Schroeder M, et al. The histone H3.3K27M mutation in pediatric glioma reprograms H3K27 methylation and gene expression. Genes Dev. 2013;27(9):985–90.
13. Louis DN, Perry A, Reifenberger G, von Deimling A, Figarella-Branger D, Cavenee WK, et al. The 2016 World Health Organization Classification of Tumors of the Central Nervous System: a summary. Acta Neuropathol. 2016;131(6):803–20.
14. Azad TD, Jin MC, Bernhardt LJ, Bettegowda C. Liquid biopsy for pediatric diffuse midline glioma: a review of circulating tumor DNA and cerebrospinal fluid tumor DNA. Neurosurg Focus. 2020;48(1):E9.
15. Williams JR, Young CC, Vitanza NA, McGrath M, Feroze AH, Browd SR, et al. Progress in diffuse intrinsic pontine glioma: advocating for stereotactic biopsy in the standard of care. Neurosurg Focus. 2020;48(1):E4.

16. Puget S, Beccaria K, Blauwblomme T, Roujeau T, James S, Grill J, et al. Biopsy in a series of 130 pediatric diffuse intrinsic Pontine gliomas. Childs Nerv Syst. 2015;31(10):1773–80.
17. Bonner ER, Bornhorst M, Packer RJ, Nazarian J. Liquid biopsy for pediatric central nervous system tumors. NPJ Precis Oncol. 2018;2(1):29.
18. Huang TY, Piunti A, Lulla RR, Qi J, Horbinski CM, Tomita T, et al. Detection of Histone H3 mutations in cerebrospinal fluid-derived tumor DNA from children with diffuse midline glioma. Acta Neuropathol Commun. 2017;5(1):28–12.
19. Panditharatna E, Kilburn LB, Aboian MS, Kambhampati M, Gordish-Dressman H, Magge SN, et al. Clinically Relevant and Minimally Invasive Tumor Surveillance of Pediatric Diffuse Midline Gliomas Using Patient-Derived Liquid Biopsy. Clin Cancer Res. 2018;24(23):5850–9.
20. Bounajem MT, Karsy M, Jensen RL. Liquid biopsies for the diagnosis and surveillance of primary pediatric central nervous system tumors: a review for practicing neurosurgeons. Neurosurg Focus. 2020;48(1):E8.
21. Hashizume R, Smirnov I, Liu S, Phillips J, Hyer J, McKnight T, et al. Characterization of a diffuse intrinsic pontine glioma cell line: implications for future investigations and treatment. J Neurooncol. 2012;110(3):305–13.
22. Takeshita I, Takaki Tosuke, Kuramitsu M, Nagasaka S, Machi T, Ogawa H, et al. Characteristics of an established human glioma cell line, KNS-42. Neurol Med Chir (Tokyo). 1987;27(7):581–7.
23. Stallard S, Savelieff MG, Wierzbicki K, Mullan B, Miklja Z, Bruzek A, et al. CSF H3F3A K27M circulating tumor DNA copy number quantifies tumor growth and in vitro treatment response. Acta Neuropathol Commun. 2018;6(1):80–4.
24. Silantyev AS, Falzone L, Libra M, Gurina OI, Kardashova KS, Nikolouzakis TK, et al. Current and Future Trends on Diagnosis and Prognosis of Glioblastoma: From Molecular Biology to Proteomics. Cells. 2019;8(8):863.
25. Tuaeva NO, Falzone L, Porozov YB, Nosyrev AE, Trukhan VM, Kovatsi L, et al. Translational Application of Circulating DNA in Oncology: Review of the Last Decades Achievements. Cells. 2019;8(10):1251.
26. De Mattos-arruda L, Mayor R, Ng CKY, Weigelt B, Martínez-ricarte F, Torrejon D, et al. Cerebrospinal fluid-derived circulating tumour DNA better represents the genomic alterations of brain tumours than plasma. Nat Commun. 2015;6(1):8839.

Figures

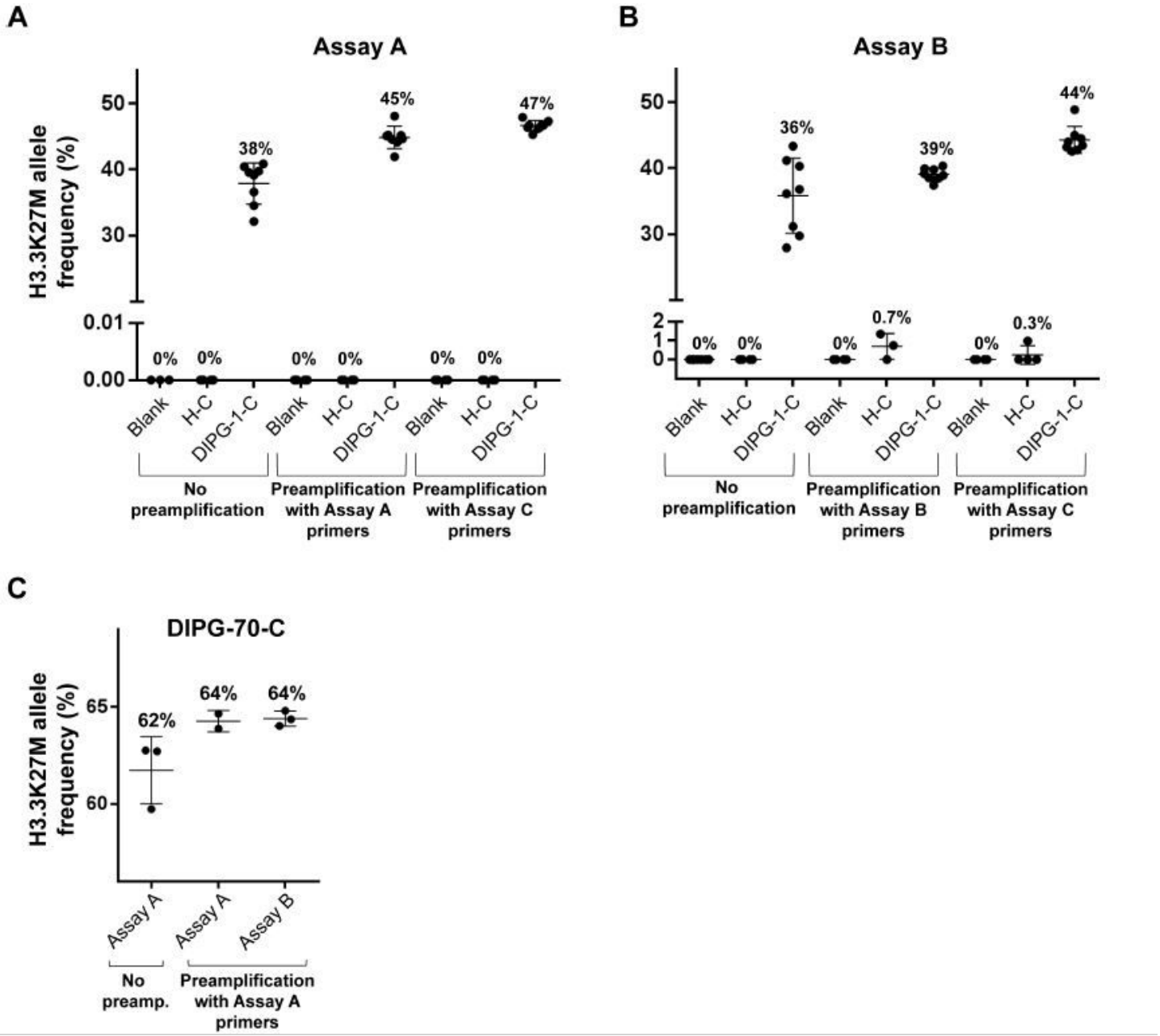

Figure 1

CSF ctDNA ddPCR analysis across platforms, with and without pre-amplification. The effect of DNA pre-amplification on BioRad platform test sensitivity was evaluated using ctDNA extracted from H3K27M mutant CSF (DIPG-1-C), non-tumor CSF (H-C) and non-template controls (blank). A. ddPCR with Assay A and B. Assay B, after PCR pre-amplification of input DNA using the same respective primer set resulted in greater droplet counts compared to ddPCR without prior DNA PCR pre-amplification. A further increase in droplet detection was achieved after DNA pre-amplification using a 300bp H3F3A primer (Assay C), with no observed change in detected MAF with either assay after pre-amplification. C. RainDance platform results. The effect of DNA pre-amplification on RainDance platform test sensitivity was evaluated using ctDNA extracted from H3K27M mutant CSF (DIPG-70-C). PCR pre-amplification of input DNA using Assay A or Assay B increased detected droplet counts, relative to ddPCR analysis alone by Assay A, with no effect on observed MAF. KEY: % values = Mutation Allelic Frequency (MAF); * = Statistically significant difference in MAF (t-test, p<.05)

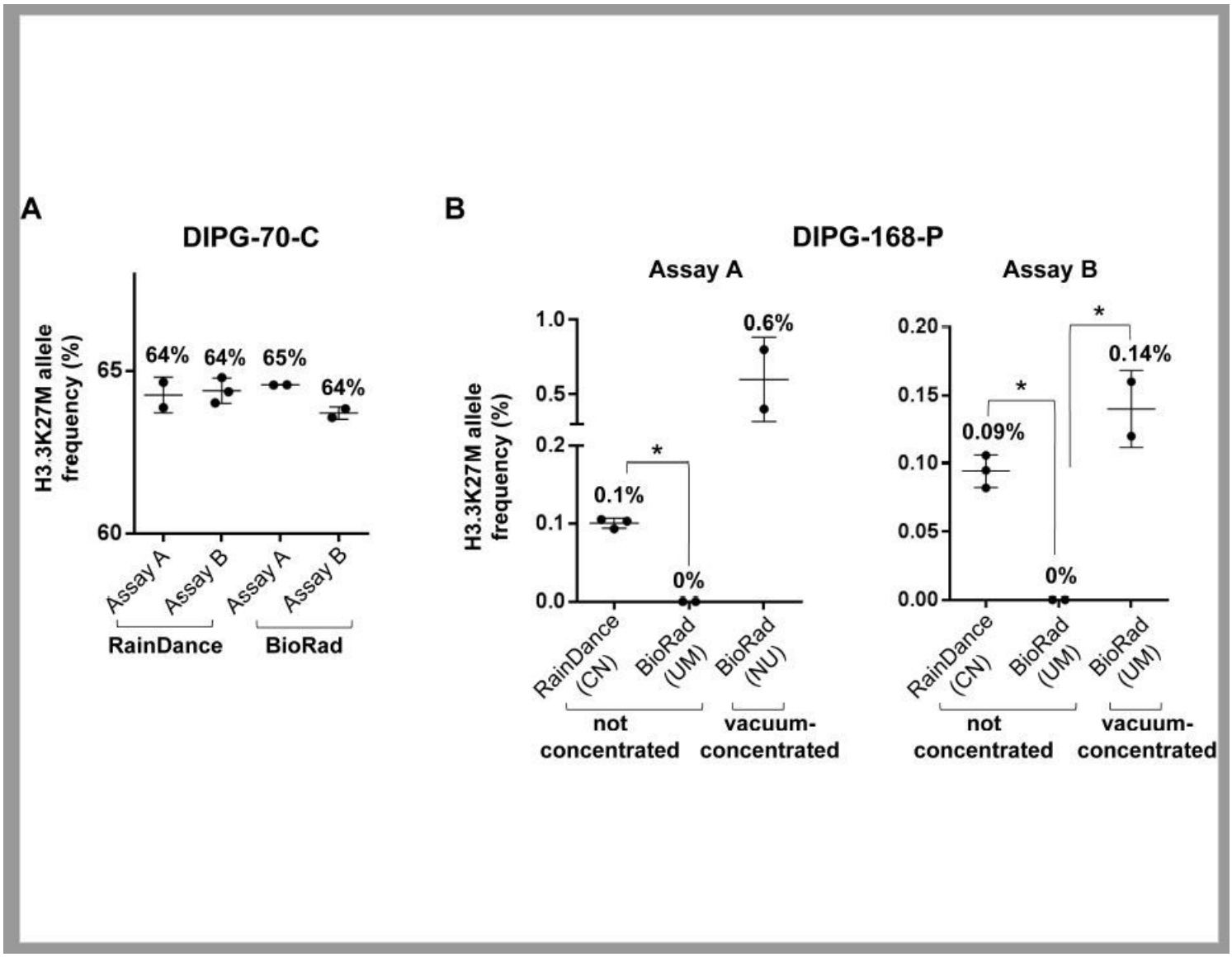

Figure 2

Optimization of ctDNA detection across technical platforms and institutions. ctDNA extracted from CSF (DIPG-70-C) and plasma (DIPG-168-P) samples were analyzed for H3K27M mutation on BioRad and RainDance platforms at multiple institutions (CN, NU, UM). A. CSF-derived ctDNA ddPCR results. CSF-derived ctDNA was pre-amplified at CN prior to ddPCR analysis. A 12µL of sample was analyzed on the RainDance platform (CN), and 1µL analyzed on the BioRad platform (UM). Fewer positive droplets were detected on the BioRad compared to the RainDance platform, while MAF remained similar across platforms and institutions. B. Plasma-derived ctDNA analysis. Plasma-derived ctDNA was pre-amplified at CN via conventional PCR, using Assay A (right) and Assay B (left) primer/ probe sets, prior to ddPCR analysis with Assay A across institutions. Speed vacuum concentration of samples was necessary to ensure preservation of input DNA in the requisite smaller sample input volume for the BioRad instrument. Superior test sensitivity was observed on the RainDance platform with both assays, while vacuum concentration increased observed MAF after Assay B ddPCR on the BioRad platform (t-test). KEY: % values = Mutation Allelic Frequency (MAF); * = Statistically significant difference in MAF (t-test, $p<.05$)

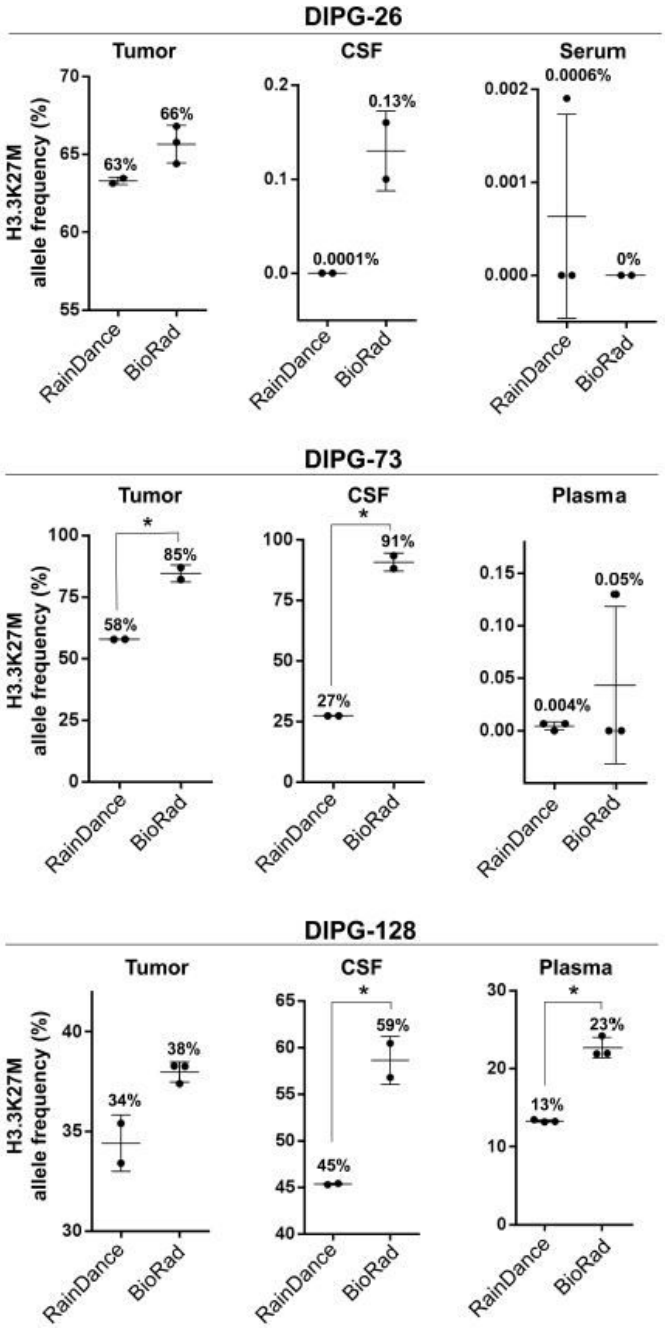

Figure 3

H3.3K27M mutant DNA is detectable in patient-matched tumor tissue, CSF and plasma serum specimens. Patient-matched specimens from children with H3K27M DMG (n=3) were analyzed on the BioRad and RainDance platforms using Assay A. Mutant droplets were detected in all specimens across each subject tested, with greater MAF observed on the BioRad platform (t-test). Due to higher extracted [ctDNA] from DIPG-128 CSF and plasma, samples were diluted 1:10 in DNA suspension buffer to prevent probe signal oversaturation. All other samples were diluted 1:5 as described. KEY: % values = Mutation Allelic Frequency (MAF); * = Statistically significant difference in MAF (t-test, p<.05).

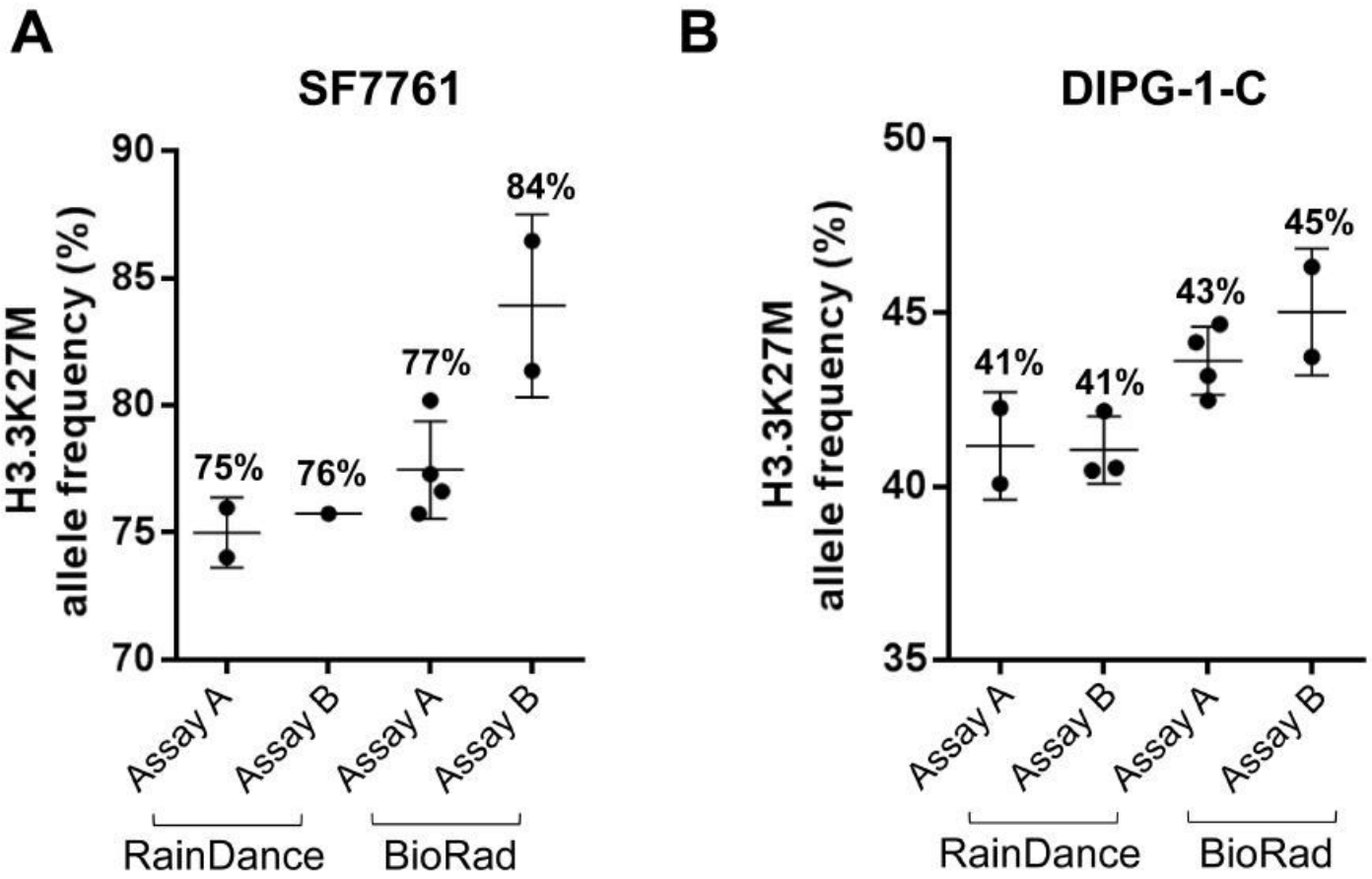

Figure 4

ddPCR results are consistent across institutions, irrespective of specimen preparation location. To determine the effects of location of sample DNA extraction and specimen shipment on ddPCR analysis results, DNA was extracted from A. H3K27M mutant DMG CSF (DIPG-1-C), and B. DMG cells (SF 7761) at NU. ctDNA was pre-amplified using Assay C primers (NU), then analyzed on BioRad (NU) and RainDance (CN) platforms, with results compared to those from ctDNA extracted at CN. As with CN-prepared specimens, NU-prepared specimens yielded greater relative positive droplet counts in cell-derived ctDNA compared to CSF, and on RainDance compared to BioRad, with consistent droplet counts and MAFs between assays within a given platform. KEY: % values = Mutation Allelic Frequency (MAF).

Supplementary Files

This is a list of supplementary files associated with this preprint. Click to download.

- AdditionalFigure1.pdf
- AdditionalFigure2.pdf
- AdditionalFigure3.pdf
- AdditionalFigure4.pdf
- AdditionalFigure5.pdf

- AdditionalTable1.docx